

# Lattice effective field theory calculations for $A = 3, 4, 6, 12$ nuclei

Evgeny Epelbaum<sup>a,b</sup>, Hermann Krebs<sup>b,a</sup>, Dean Lee<sup>c,b</sup>, Ulf-G. Meißner<sup>b,a,d</sup>

<sup>a</sup>*Institut für Kernphysik (IKP-3) and Jülich Center for Hadron Physics,  
Forschungszentrum Jülich, D-52425 Jülich, Germany*

<sup>b</sup>*Helmholtz-Institut für Strahlen- und Kernphysik (Theorie) and  
Bethe Center for Theoretical Physics,  
Universität Bonn, D-53115 Bonn, Germany*

<sup>c</sup>*Department of Physics, North Carolina State University,  
Raleigh, NC 27695, USA*

<sup>d</sup>*Institute for Advanced Simulation (IAS),  
Forschungszentrum Jülich, D-52425 Jülich, Germany*

We present lattice results for the ground state energies of tritium, helium-3, helium-4, lithium-6, and carbon-12 nuclei. Our analysis includes isospin-breaking, Coulomb effects, and interactions up to next-to-next-to-leading order in chiral effective field theory.

PACS numbers: 21.10.Dr, 21.30.-x, 21.45.-v, 21.60.De

Several ab initio approaches have been used to calculate the properties of various few- and many-nucleon systems. Some recent work includes the no-core shell model [1–5], constrained-path [6–9] and fixed-node [10, 11] Green’s function Monte Carlo, auxiliary-field diffusion Monte Carlo [12–14], and coupled cluster methods [15–17]. The diversity of methods is useful since each technique has its own computational scaling, systematic errors, and range of accessible problems. Furthermore, quantities not directly measured in experiments can be benchmarked with calculations using other methods.

Another ab initio approach in the recent literature is lattice effective field theory. This method combines the theoretical framework of effective field theory (EFT) with numerical lattice methods. When compared with other methods it is unusual in that all systematic errors are introduced up front when defining the truncated low-energy effective theory. This eliminates approximation errors tied with a specific calculational tool, physical system, or observable. By including higher-order interactions in the low-energy effective theory, one can reasonably expect systematic and systemic improvement for all low-energy observables. The approach has been used to simulate nuclear matter [18] and neutron matter [19–24]. The method has also been applied to nuclei with  $A \leq 4$  in pionless EFT [25] and chiral EFT [26, 27]. A review of lattice effective field theory calculations can be found in Ref. [28].

In this letter we present the first lattice calculations for lithium-6 and carbon-12 using chiral effective field theory. We address a fundamental question in the nuclear theory community: Can effective field theory be applied to nuclei beyond the very lightest? While there are several calculations that probe this question using interactions derived from chiral effective field theory, we present the first calculations posed and computed entirely within the framework of effective field theory. Our results show

that lattice-regularized effective field theory can be applied to the ground state of carbon-12. Furthermore there is a clear path towards larger nuclei and nuclear matter. We also describe the first lattice calculations to include isospin-breaking and Coulomb interactions, and compute the energy splitting between helium-3 and the triton. Our discussion focuses on new features of the calculation and new results. A complete description of the calculational method is contained in a separate paper [29].

The low-energy expansion in effective field theory is organized in powers of  $Q/\Lambda$ , where  $Q$  is the low momentum scale associated with external nucleon momenta or the pion mass, and  $\Lambda$  is the high momentum scale at which the effective theory breaks down. Some reviews of chiral effective field theory can be found in Ref. [30–33]. At leading order (LO) in the Weinberg power counting scheme the nucleon-nucleon effective potential contains two independent contact interactions and instantaneous one-pion exchange. As in previous lattice studies we make use of an “improved” leading-order action. This improved leading-order action is treated completely non-perturbatively, while higher-order interactions are included as a perturbative expansion in powers of  $Q/\Lambda$ .

We use the improved  $\text{LO}_3$  lattice action introduced in Ref. [23] with spatial lattice spacing  $a = (100 \text{ MeV})^{-1} = 1.97 \text{ fm}$  and temporal lattice spacing  $a_t = (150 \text{ MeV})^{-1} = 1.32 \text{ fm}$ . The interactions provide a good description of the neutron-proton  $S$ -wave and  $P$ -wave phase shifts at low energies as well as the  $S$ - $D$  mixing angle. Plots of the scattering data for the  $\text{LO}_3$  lattice action can be found in Ref. [23]. The corrections at next-to-leading order (NLO) and next-to-next-to-leading order (NNLO) are calculated using perturbation theory. A description of these interactions on the lattice is documented in Ref. [27].

At NLO there are corrections to the two leading-order

coefficients and seven additional unknown coefficients for operators with two powers of momentum. These nine coefficients are determined by fitting to the neutron-proton  $S$ -wave and  $P$ -wave phase shifts and  $S$ - $D$  mixing angle at low energies. At NNLO there are two additional cutoff-dependent coefficients associated with three-nucleon interactions. These are parameterized by two dimensionless coefficients  $c_D$  and  $c_E$ , corresponding with the three-nucleon one-pion exchange diagram and three-nucleon contact interaction respectively. We constrain  $c_E$  by requiring that the triton energy equals the physical value of  $-8.48$  MeV. However the parameter  $c_D$  is relatively unconstrained by low-energy phenomena such as the deuteron-neutron spin-doublet phase shifts. Currently we are investigating other methods for constraining  $c_D$ , including one recent suggestion to determine  $c_D$  from the triton beta decay rate [34]. In this analysis we simply use the estimate  $c_D \sim O(1)$  and check the dependence of observables upon changes in  $c_D$ .

In addition to isospin-symmetric interactions, we also include isospin-breaking (IB) and electromagnetic (EM) interactions. Isospin violation in effective field theory has been addressed extensively in the literature [35–40]. In the counting scheme proposed in Ref. [40], the isospin-breaking one-pion exchange interaction and Coulomb potential are numerically the same size as  $O(Q^2/\Lambda^2)$  corrections at NLO. On the lattice we treat the Coulomb potential in position space with the usual  $\alpha_{EM}/r$  dependence. However this definition is singular for two protons on the same lattice site and requires short-distance renormalization via a proton-proton contact interaction. In this study we include all possible contact interactions, namely interactions for neutron-neutron, proton-proton, spin-singlet neutron-proton, and spin-triplet neutron-proton. The two neutron-proton contact interactions are already included at NLO and determined from neutron-proton scattering. The other two coefficients are determined from fitting to  $S$ -wave phase shifts for proton-proton scattering and the neutron-neutron scattering length. Details of this calculation will be presented in a separate paper [29].

The first results we present are for helium-3 and the triton. The three-nucleon system is sufficiently small that we can use iterative sparse-matrix eigenvector methods to compute helium-3 and the triton on cubic periodic lattices. We consider cubes with side lengths  $L$  up to 16 fm and extract the infinite volume limit using the asymptotic parameterization [41],  $E(L) \approx E(\infty) - ce^{-L/L_0}/L$ . While the triton energy at infinite volume is used to set the unknown coefficient  $c_E$ , the energy splitting between helium-3 and the triton is a prediction that can be compared with experiment. The energy difference between helium-3 and the triton is plotted in Fig. 1 as a function of cube length. We show several different asymptotic fits using different subsets of data points. To the order at which we are working there is no dependence of

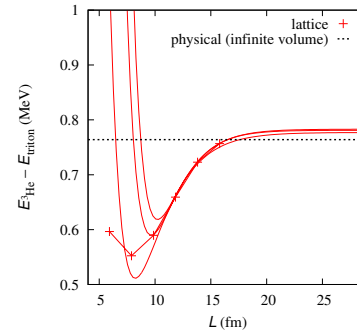


FIG. 1: Plot of the energy difference between helium-3 and the triton as a function of periodic cube length.

the energy splitting upon the value of  $c_D$ . Our calculations at next-to-next-to-leading order give a value of 0.780 MeV with an infinite-volume extrapolation error of  $\pm 0.003$  MeV. To estimate other errors we take into account an uncertainty of  $\pm 1$  fm in the neutron scattering length and a 5% relative uncertainty in our lattice fit of the splitting between neutron-proton and proton-proton phase shifts at low energies. Our final result for the energy splitting with error bars is 0.78(5) MeV. This agrees well with the experimental value of 0.76 MeV.

For systems with more than three nucleons, we use projection Monte Carlo with auxiliary fields and extract the properties of the ground state using Euclidean-time projection. The transfer matrix,  $M$ , is the normal-ordered exponential of the Hamiltonian over one temporal lattice spacing. As in previous lattice Monte Carlo simulations we first define a transfer matrix  $M_{\text{SU}(4)\pi}$  which is invariant under Wigner’s  $\text{SU}(4)$  symmetry rotating all spin and isospin components of nucleons. This transfer matrix acts as an approximate low-energy filter that happens to be computationally inexpensive. Starting from a Slater determinant of free-particle standing waves,  $|\Psi^{\text{free}}\rangle$ , we construct the trial state  $|\Psi(t')\rangle$  by successive multiplication,

$$|\Psi(t')\rangle = (M_{\text{SU}(4)\pi})^{L_{t_o}} |\Psi^{\text{free}}\rangle, \quad (1)$$

where  $t' = L_{t_o} a_t$  and  $L_{t_o}$  is the number of “outer” time steps. The trial function  $|\Psi(t')\rangle$  is then used as the starting point for the calculation. The amplitude  $Z(t)$  is defined as

$$Z(t) = \langle \Psi(t') | (M_{\text{LO}})^{L_{t_i}} | \Psi(t') \rangle, \quad (2)$$

where  $t = L_{t_i} a_t$  and  $L_{t_i}$  is the number of “inner” time steps. The transient energy  $E(t)$  is proportional to the logarithmic derivative of  $Z(t)$ , and the ground state energy is given by the limit of  $E(t)$  as  $t \rightarrow \infty$ . Each of the transfer matrices are functions of the auxiliary fields and pion fields, and the Monte Carlo integration over field configurations is performed using hybrid Monte

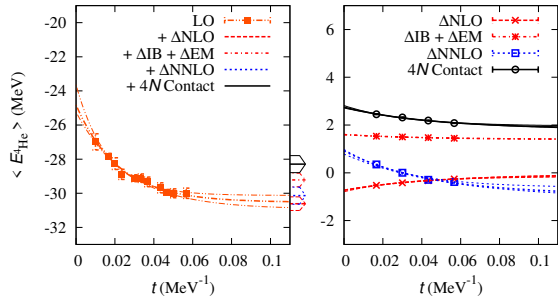


FIG. 2: Ground state energy for helium-4 as a function of Euclidean time projection.

Carlo. Contributions due to NLO and NNLO interactions, isospin breaking (IB), and electromagnetic interactions (EM) are incorporated using perturbation theory.

In Fig. 2 we show lattice results for the ground state of helium-4 in a periodic cube of length 9.9 fm. For the numerical extrapolation in Euclidean time we use the decaying exponential functions described in Ref. [27]. The plot on the left shows the contributions from leading-order and higher-order contributions added cumulatively. The plot on the right shows the higher-order corrections separately. For each case we show the best fit as well as the one standard-deviation bound. We estimate this bound by generating an ensemble of fits determined with added random Gaussian noise proportional to the error bars of each data point and varying the number of fitted data points. These results are similar to those found in Ref. [27] using the  $\text{LO}_2$  action. For  $c_D = 1$  we get  $-30.5(4)$  MeV at LO,  $-30.6(4)$  MeV at NLO,  $-29.2(4)$  MeV at NLO with IB and EM corrections, and  $-30.1(5)$  MeV at NNLO. The helium-4 energy decreases  $0.4(1)$  MeV for each unit increase in  $c_D$ .

The size of the corrections at NNLO gives an estimate of the remaining error from higher-order terms in the effective field theory expansion. Given our cutoff momentum scale of  $\Lambda = \pi/a = 314$  MeV, an error of 1 to 2 MeV is consistent with the expected size of higher-order contributions. Interactions at higher order than NNLO are beyond the scope of the current calculation. However if it happens that the higher-order effects are most important when all four nucleons are in close proximity, then we should see universal behavior which can be reproduced by an effective four-nucleon contact interaction. We test this universality hypothesis by introducing an effective four-nucleon contact interaction tuned to reproduce the physical helium-4 energy of  $-28.3$  MeV. The contribution of this interaction in helium-4 is shown in Fig. 2.

In Fig. 3 we show lattice results for the ground state of lithium-6 in a periodic cube of length 9.9 fm. For  $c_D = 1$

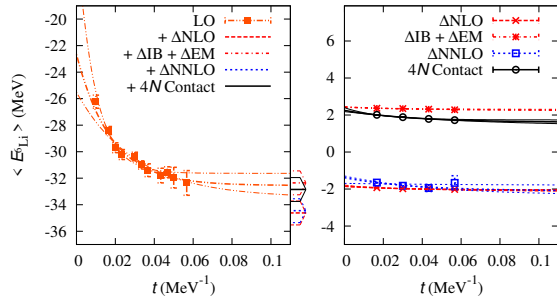


FIG. 3: Ground state energy for lithium-6 as a function of Euclidean time projection.

we get  $-32.6(9)$  MeV at LO,  $-34.6(9)$  MeV at NLO,  $-32.4(9)$  MeV at NLO with IB and EM corrections, and  $-34.5(9)$  MeV at NNLO. Adding the contribution of the effective four-nucleon interaction to the NNLO result gives  $-32.9(9)$  MeV. This lies within error bars of the physical value  $-32.0$  MeV. However we expect some overbinding due to the finite periodic volume, and the deviation of  $0.9$  MeV is consistent with the expected size of the finite volume correction. Further calculations at varying volumes will be needed to determine this volume dependence. Without the effective four-nucleon interaction, the lithium-6 energy decreases  $0.7(1)$  MeV for each unit increase in  $c_D$ . With the effective four-nucleon interaction the lithium-6 energy decreases  $0.35(5)$  MeV per unit increase in  $c_D$ .

In Fig. 4 we show lattice results for the ground state of carbon-12 in a periodic cube of length 13.8 fm. For  $c_D = 1$  we get  $-109(2)$  MeV at LO,  $-115(2)$  MeV at NLO,  $-108(2)$  MeV at NLO with IB and EM corrections, and  $-106(2)$  MeV at NNLO. Adding the contribution of the effective four-nucleon interaction to the NNLO result gives  $-99(2)$  MeV. This is an overbinding of 7% from the physical value,  $-92.2$  MeV. We note that an overbinding of 7% is actually a reasonable estimate of the finite volume correction for carbon-12 in a periodic box of length 13.8 fm. This suggests that at infinite volume the error is significantly smaller than 7%. Further calculations at varying volumes will be needed to measure the volume dependence. Without the effective four-nucleon interaction, the carbon-12 energy decreases  $1.7(3)$  MeV for each unit increase in  $c_D$ . With the effective four-nucleon interaction the carbon-12 energy decreases  $0.3(1)$  MeV per unit increase in  $c_D$ .

The results for lithium-6 and carbon-12 appear to confirm the universality hypothesis regarding higher-order interactions. The much reduced dependence upon  $c_D$  is also consistent with the universality hypothesis. The effective four-nucleon contact interaction can be viewed as absorbing the dependence on  $c_D$ . We note a re-

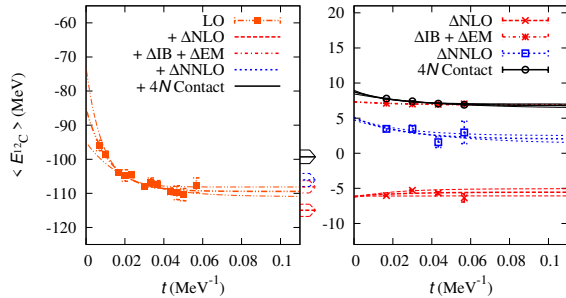


FIG. 4: Ground state energy for carbon-12 as a function of Euclidean time projection.

cent related paper on the renormalization group evolution of higher-nucleon interactions [42]. The accuracy of these lattice calculations are competitive with recent calculations obtained using other ab initio methods. Constrained-path Green's function Monte Carlo calculations and no-core shell model calculations have an accuracy of 1% – 2% in energy for nuclei  $A \leq 12$ . Coupled cluster calculations without three-nucleon interactions are accurate to within 1 MeV per nucleon for medium mass nuclei. Future lattice studies should look at probing large volumes, including higher-order effects, and decreasing the lattice spacing.

Lattice effective field theory combines the generality of effective field theory with the flexibility of lattice methods. The computational scaling of the calculations presented here indicates that larger systems with more nucleons should be possible. By applying different lattice boundary conditions in the spatial and temporal directions, it is possible to probe nuclear systems of many different varieties: few-body and many-body systems; zero temperature and nonzero temperature; nuclear matter, neutron matter, and asymmetric nuclear matter.

*Partial financial support provided by the Deutsche Forschungsgemeinschaft, Helmholtz Association, U.S. Department of Energy, and EU HadronPhysics2 Project. Computational resources provided by the Jülich Supercomputing Centre.*

[1] C. Forssen, P. Navratil, W. E. Ormand, and E. Caurier, Phys. Rev. **C71**, 044312 (2005).  
 [2] A. Nogga, P. Navratil, B. R. Barrett, and J. P. Vary, Phys. Rev. **C73**, 064002 (2006).  
 [3] I. Stetcu, B. R. Barrett, and U. van Kolck, Phys. Lett. **B653**, 358 (2007).  
 [4] P. Navratil, V. G. Gueorguiev, J. P. Vary, W. E. Ormand, and A. Nogga, Phys. Rev. Lett. **99**, 042501 (2007).  
 [5] P. Maris, J. P. Vary, and A. M. Shirokov, Phys. Rev.

**C79**, 014308 (2009).  
 [6] S. C. Pieper, K. Varga, and R. B. Wiringa, Phys. Rev. **C66**, 044310 (2002).  
 [7] S. C. Pieper, Nucl. Phys. **A751**, 516 (2005).  
 [8] L. E. Marcucci, M. Pervin, S. C. Pieper, R. Schiavilla, and R. B. Wiringa (2008), arXiv:0810.0547.  
 [9] S. C. Pieper, B. Am. Phys. Soc. **54**, 70 (2009).  
 [10] S. Y. Chang et al., Nucl. Phys. **A746**, 215 (2004).  
 [11] A. Gezerlis and J. Carlson, Phys. Rev. **C77**, 032801 (2008); arXiv:0911.3907.  
 [12] S. Gandolfi, F. Pederiva, S. Fantoni, and K. E. Schmidt, Phys. Rev. Lett. **99**, 022507 (2007).  
 [13] S. Gandolfi, A. Y. Illarionov, K. E. Schmidt, F. Pederiva, and S. Fantoni (2009), arXiv:0903.2610.  
 [14] S. Gandolfi et al. (2009), arXiv:0909.3487.  
 [15] M. Wloch et al., Phys. Rev. Lett. **94**, 212501 (2005).  
 [16] G. Hagen, D. J. Dean, M. Hjorth-Jensen, T. Papenbrock, and A. Schwenk, Phys. Rev. **C76**, 044305 (2007).  
 [17] G. Hagen, T. Papenbrock, D. J. Dean, and M. Hjorth-Jensen, Phys. Rev. Lett. **101**, 092502 (2008).  
 [18] H. M. Müller, S. E. Koonin, R. Seki, and U. van Kolck, Phys. Rev. **C61**, 044320 (2000).  
 [19] D. Lee and T. Schäfer, Phys. Rev. **C72**, 024006 (2005).  
 [20] D. Lee, B. Borasoy, and T. Schäfer, Phys. Rev. **C70**, 014007 (2004).  
 [21] T. Abe and R. Seki, Phys. Rev. **C79**, 054002 (2009).  
 [22] B. Borasoy, E. Epelbaum, H. Krebs, D. Lee, and U.-G. Meißner, Eur. Phys. J. **A35**, 357 (2008).  
 [23] E. Epelbaum, H. Krebs, D. Lee, and U.-G. Meißner, Eur. Phys. J. **A40**, 199 (2009).  
 [24] G. Wlazowski and P. Magierski (2009), arXiv:0912.0373.  
 [25] B. Borasoy, H. Krebs, D. Lee, and U.-G. Meißner, Nucl. Phys. **A768**, 179 (2006).  
 [26] B. Borasoy, E. Epelbaum, H. Krebs, D. Lee, and U.-G. Meißner, Eur. Phys. J. **A31**, 105 (2007).  
 [27] E. Epelbaum, H. Krebs, D. Lee, and U. G. Meißner, Eur. Phys. J. **A41**, 125 (2009).  
 [28] D. Lee, Prog. Part. Nucl. Phys. **63**, 117 (2009).  
 [29] E. Epelbaum, H. Krebs, D. Lee, and U.-G. Meißner (2010), in preparation.  
 [30] U. van Kolck, Prog. Part. Nucl. Phys. **43**, 337 (1999).  
 [31] P. F. Bedaque and U. van Kolck, Ann. Rev. Nucl. Part. Sci. **52**, 339 (2002).  
 [32] E. Epelbaum, Prog. Part. Nucl. Phys. **57**, 654 (2006).  
 [33] E. Epelbaum, H.-W. Hammer, and U.-G. Meißner, Rev. Mod. Phys. **81**, 1773 (2010).  
 [34] D. Gazit, S. Quaglioni, and P. Navratil, Phys. Rev. Lett. **103**, 102502 (2009).  
 [35] U. van Kolck, J. L. Friar, and J. T. Goldman, Phys. Lett. **B371**, 169 (1996).  
 [36] U. van Kolck, M. C. M. Rentmeester, J. L. Friar, J. T. Goldman, and J. J. de Swart, Phys. Rev. Lett. **80**, 4386 (1998).  
 [37] E. Epelbaum and U.-G. Meißner, Phys. Lett. **B461**, 287 (1999).  
 [38] M. Walz, U. G. Meißner, and E. Epelbaum, Nucl. Phys. **A693**, 663 (2001).  
 [39] J. L. Friar, U. van Kolck, G. L. Payne, and S. A. Coon, Phys. Rev. **C68**, 024003 (2003).  
 [40] E. Epelbaum and U.-G. Meißner, Phys. Rev. **C72**, 044001 (2005).  
 [41] M. Lüscher, Commun. Math. Phys. **104**, 177 (1986).  
 [42] E. D. Jurgenson, P. Navratil, and R. J. Furnstahl, Phys. Rev. Lett. **103**, 082501 (2009).